frontiers in Materials

ORIGINAL RESEARCH
published: 03 January 2022
doi: 10.3389/fmats.2021.792714

The Establishment of Thermodynamic Model for Ti Bearing Steel-Slag Reaction and Discuss

Mao-Guo Zhao[1], *Xu-Feng Wang*[1], *Gu-Jun Chen*[2] *and Sheng-Ping He*[1]*

[1]School of Materials Science and Engineering, Chongqing University, Chongqing, China, [2]School of Materials Science and Engineering, Yangtze Normal University, Fuling, China

A thermodynamic model for seven CaO-MgO-BaO-CaF_2-SiO_2-Al_2O_3-TiO_2 ladle slags based on the Ion and Molecule Coexistence theory (IMCT) is establishment and validated by the experiment results at 1873K. The calculated activity of SiO_2, Al_2O_3 and TiO_2 in the slag can be approved by the experiment results and the IMCT model used in this study is reasonable. Then the influence factors such as the mass ratio of CaO to SiO_2 (C/S ratio) ranging from 1 to 10, the mass ratio of CaO to Al_2O_3 (C/A ratio) ranging from 1 to 2.5, TiO_2 content (wt pct) ranging from 0 to 30, BaO content (wt pct) ranging from 0 to 30 are investigated based on the thermodynamic calculating results. The raise of C/S ratio, TiO_2 content and BaO content in the slag can increase the molar Gibbs energy change (ΔG) of Ti reacted with SiO_2 and Al_2O_3 or Al reacted with SiO_2. The effect of C/A ratio on the molar Gibbs energy change (ΔG) of Ti reacted with SiO_2 and Al_2O_3 or Al reacted with SiO_2 was less. Finally, the slag with higher C/S ratio and TiO_2 content and appropriate BaO content can weaken the reaction between Ti and SiO_2 or Al_2O_3 in the slag.

Keywords: thermodynamic model, Ti-bearing steel, slag, IMCT, ladel

OPEN ACCESS

Edited by:
Antonio Caggiano, Darmstadt University of Technology, Germany

Reviewed by:
Il Sohn, Yonsei University, South Korea
Qifeng Shu, University of Oulu, Finland

***Correspondence:**
Sheng-Ping He
heshp@cqu.edu.cn

Specialty section:
This article was submitted to Structural Materials, a section of the journal Frontiers in Materials

Received: *11 October 2021*
Accepted: *15 November 2021*
Published: *03 January 2022*

Citation:
Zhao M-G, Wang X-F, Chen G-J and He S-P (2022) The Establishment of Thermodynamic Model for Ti Bearing Steel-Slag Reaction and Discuss. Front. Mater. 8:792714. doi: 10.3389/fmats.2021.792714

INTRODUCTION

TiC and TiN inclusion can be formed in the Ti bearing steel in the solidification process (Cavazos et al., 2011; Leban and Tisu, 2013), which can increase the strength of the final products, as the steel's secondary phase (Huang et al., 2018). During the initial solidification period, the heterogeneous nucleation of delta ferrite could formed on the TiN inclusions and then the equiaxed fine-grained structure was generated (Fujimura et al., 2001). For this reason, the addition of titanium to the liquid steel in the ladle for improving properties has increased in recent years. Nevertheless the loss of Ti will persist in the ladle metallurgy process, mainly oxidized by the slag. Then the formed TiO_x in the steel would reacted with Mg, Ca or Al_2O_3 in the steel and the complex inclusions such as $MgAl_2O_4$ spinal and MgO-TiO_x spinal, surrounded by TiN and perovskite are formed. This would lead to the clogging of submerged nozzle and forming of surface defects on the steel products (Maddalena et al., 2000; Nunnington and Sutcliffe, 2001; Zheng et al., 2004). Thus, in order to obtain an optimal slag composition for the ladle refining of Al-killed and Ti bearing steel, it is important to investigate the reaction between slag and molten steel.

Kim et al. (1993) found that the SiO_2 in the slag could oxidize the Titanium in the liquid steel. Park et al. (2004) also found that Aluminum and Titanium could be simultaneously oxidized by the SiO_2 in the 14%CaO-35%Al_2O_3-10%MgO-%4SiO_2 slag and the soluble oxygen was supersaturated during the course, particularly with respect to Al. Then the re-oxidation mechanism of Al and Ti in the liquid steel by SiO_2 was depicted in **Figure 1**. It can be seen from **Figure 1**, the oxidation process of Al or Ti mainly

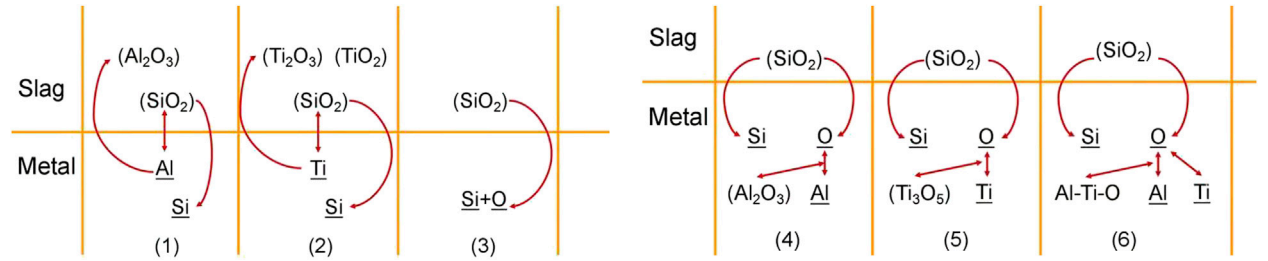

FIGURE 1 | The main mechanism for the re-oxidation of Ti and Al in metal.

include two ways, on the one hand, the Al or Ti in the metal reacted with the SiO_2 in the slag directly; on the other hand, the SiO_2 in the slag decomposed of Si and O, then they transferred to the liquid steel and oxidized the Al and Ti in the liquid steel. Park et al. (2009) also investigate the thermodynamic behavior of TiO_x in the refining slag (CaO-SiO_2-MgO-Al_2O_3-TiO_x

-CaF_2) equilibrated with Fe-11%Cr melts. They found that the equilibrium between silicon and titanium in steel melts and their oxides in the slags are theoretically expected and experimentally proved well. They also calculated the relationship between Aluminum and Titanium in the steel melts and their oxides in the slag. The slope of the line is 0.5, which is lower than 1. Therefore, they summarized that the activity coefficient of TiO_x in the slag would be affected in the composition range investigated in their study. They also found that with the increase of $(\%SiO_2)/(\%SiO_2+\%Al_2O_3)$ in the slag, the activity coefficient of TiO_2 gradually decreased. The attraction between TiO_2 and SiO_2 is greater than that between TiO_2 and Al_2O_3 in the present slag system due to the electronegativity difference between each cation involved. The activity of TiO2 in the slag system containing 10% MgO shows a negative deviation from an ideality, while that in the CaO-SiO_2-Al_2O_3-MgO_{satd}-CaF_2 system is really close to the ideal behavior up to about $x_{TiO_2} = 0.1$. This is mainly due to the relatively basic characteristic of TiO_2.

Qian et al. (2014) found that when the TiO_2 content in the slag reached to 8%, the oxidation of Ti in the Ti-stabilized stainless steel was minimum and the T. O (Total O in the steel) was constant with the time increase. They also found the influence of TiO_2 adding to the slag on the oxidation rate change of Al has an opposite tendency compared with Ti. The activity change behavior of TiO_2 in different TiO_2 content slag, calculated by IMCT model, are in good agreement of the experiment results. Li and Cheng (2019) investigated the effect of the CaF_2 contents in the CaO-SiO_2- MgO-Al_2O_3-TiO_2-CaF_2 slag on the formation of inclusion in Ti-Stabilized 20Cr Stainless Steel. They found that with the increase of CaF_2 content in the slag, the equilibrium content of Ti and Mg in the steel increased. When the CaF_2 content in the slag changed from 0 to 9.57, the equilibrium content of Ti changed from 0.018 to 0.031% and the equilibrium content of Mg changed from 12ppm to 23ppm. Due to the increase of CaF_2 content in the slag can decrease the $\lg(a_{TiO_2}/a_{SiO_2})$ and $\lg(a_{TiO_2}/a_{Al_2O_3}^{2/3})$, which would make the steel has higher Ti after the Slag-metal reaction reached to the equilibrium state. They suggested the optimal CaF_2 content in the slag was 5–10%. Meanwhile they also investigated the dependence of the composition ratio of steel on the activity ratio of slag at different CaF_2 contents, which was calculated by IMCT model, and the phenomena was found that the calculation results are consistent with the experimental results. Although the Ti could be oxidized by the SiO_2 according to the literature (Kim et al., 1993)˜ (Li and Cheng, 2019), Ti would be oxidized by Al_2O_3 in other slags, such as ESR slag (Jiang et al., 2016). And they also obtained that clearly the calculated results by IMCT model are in good agreement with experimental results. Some previous reports found that the reaction between Ti and Al_2O_3 in the slag can also cause the loss of Ti in the steel (Bomberger and Froes, 1984; Carmack et al., 1996; Jiang, 2000; Li, 2010; Jiang et al., 2016).

According to the previous researches (Qian et al., 2014; Jiang et al., 2016; Li and Cheng, 2019), The IMCT model has been applied in CaO-SiO_2-MgO-Al_2O_3-TiO_2-CaF_2 slag system successfully for Ti-bearing stainless steel and 825 alloy refining process. However, the CaO-SiO_2-MgO-Al_2O_3-TiO_2-CaF_2-BaO slag for low alloy high Ti-bearing steel refining, has never been explored. Due to the adding of BaO in the ladle slag has a excellently ability for desulphurization (Gao et al., 2012), Therefore this study is mainly focused on the investigation of the reactive between CaO-SiO_2-MgO-Al_2O_3-TiO_2-CaF_2-BaO slag and 0.361% Ti bearing steel (0.0361%Al) by use the thermodynamic model (IMCT model), which is needed to be approved by the experiment results.

THERMODYNAMIC INTERACTION FOR METAL-SLAG

The composition of Al-killed and Ti-bearing steel used in this study was listed in **Table 1**. During the ladle metallurgy process, the reactions (1–3) between the liquid steel and slag would lead to the loss of Ti and Al in the steel (Qian et al., 2014; Li and Cheng, 2019). The slag composition assigned for this paper's discussion section is shown in **Table 2**.

$$[Al] + \tfrac{3}{4}(SiO_2) = \tfrac{3}{4}[Si] + \tfrac{1}{2}(Al_2O_3) \text{ Reaction 1}$$

$$K_1 = \frac{a_{Si}^{3/4} \cdot a_{Al_2O_3}^{1/2}}{a_{Al} \cdot a_{SiO_2}^{3/4}} = \frac{f_{Si}^{3/4} \cdot [Si]^{3/4} \cdot a_{Al_2O_3}^{1/2}}{f_{Al} \cdot [Al] \cdot a_{SiO_2}^{3/4}} \quad (1)$$

$$\Delta G_1^0 = -164575 + 26.8T \quad (2)$$

TABLE 1 | The chemical composition of Al-killed and Ti-bearing liquid steel, wt pct.

Steel	C	Al	Mn	Si	P	S	Cr	Mo	Ni	Ti	N	O
A	0.178	0.039	1.210	0.191	0.005	0.003	0.114	0.198	0.078	0.361	0.004	0.006

TABLE 2 | the design slag composition used for this paper's discussion section.

Slag	C/S ratio	C/A ratio	Al_2O_3(wt pct)	BaO (wt pct)	MgO(wt pct)	CaF_2(wt pct)	TiO_2(wt pct)
S1	1–10	-	25	0	6	5	5
S2	6–10	1–2.5	-	0	6	5	5
S3	6–10	1.7	-	0	6	5	0–30
S4	6–10	1.7	-	0–30	6	5	15–25

TABLE 3 | Interaction parameters used in this paper (Hino, 2009).

e_{ij} (r_{ij})	C	Si	Mn	P	S	Mo	Al	Ti	O
Al	0.091	0.056	0.035	0.033	0.035	-	0.038	0.004	-1.98 (39.82)
Si	0.180	0.132	0.002	0.110	0.056	2.36	-0.058	-0.013	-0.23
Ti	0.165	-0.025	-0.043	0.0064	-0.11	-	0.0037	0.048	-1.80 (-0.36)

$$\lg(K_1) = \frac{8596.75}{T} - 1.40 \tag{3}$$

$$\lg\frac{[Si]^{3/4}}{[Al]} = \lg\frac{f_{Al}}{f_{Si}^{\frac{3}{4}}} + \lg\frac{a_{SiO_2}^{3/4}}{a_{Al2O3}^{1/2}} + \lg K_1 = \lg\frac{f_{Al}}{f_{Si}^{3/4}} + \lg\frac{a_{SiO_2}^{3/4}}{a_{Al2O3}^{1/2}} + \frac{8596.75}{T} - 1.40 \tag{4}$$

$[Ti] + (SiO_2) = [Si] + (TiO_2)$ Reaction 2

$$K_2 = \frac{a_{Si}\cdot a_{TiO_2}}{a_{Ti}\cdot a_{SiO_2}} = \frac{f_{Si}\cdot[Si]\cdot a_{TiO_2}}{f_{Ti}\cdot[Ti]\cdot a_{SiO_2}} \tag{5}$$

$$\Delta G_2^0 = -3503.9 - 26.03T \tag{6}$$

$$\lg(K_2) = \frac{183}{T} + 1.36 \tag{7}$$

$$\lg\frac{[Si]}{[Ti]} = \lg\frac{f_{Ti}}{f_{Si}} + \lg\frac{a_{SiO_2}}{a_{TiO_2}} + \lg K_2 = \lg\frac{f_{Ti}}{f_{Si}} + \lg\frac{a_{SiO_2}}{a_{TiO_2}} + \frac{183}{T} + 1.36 \tag{8}$$

$[Ti] + \frac{2}{3}(Al_2O_3) = \frac{4}{3}[Al] + (TiO_2)$ Reaction 3

$$K_3 = \frac{a_{Al}^{4/3}\cdot a_{TiO_2}}{a_{Ti}\cdot a_{Al_2O_3}^{2/3}} = \frac{f_{Al}^{4/3}\cdot[Al]^{4/3}\cdot a_{TiO_2}}{f_{Ti}\cdot[Ti]\cdot a_{Al_2O_3}^{2/3}} \tag{9}$$

$$\Delta G_3^0 = 225300 - 63.44T \tag{10}$$

$$\lg(K_3) = -\frac{35300}{T} + 9.94 \tag{11}$$

$$\lg\frac{[Al]^{4/3}}{[Ti]} = \lg\frac{f_{Ti}}{f_{Al}^{4/3}} + \lg\frac{a_{Al_2O_3}^{2/3}}{a_{TiO_2}} + \lg K_3 = \lg\frac{f_{Ti}}{f_{Al}^{4/3}} + \lg\frac{a_{Al_2O_3}^{2/3}}{a_{TiO_2}} - \frac{35300}{T} + 9.94 \tag{12}$$

From **Eqs. 1–12**, K_n is equilibrium constant of reaction (i); a_M is the activity of element i in the liquid steel with respect to an infinite dilute of one mass% state and is calculated by **Eq. 13**; f_M is the activity coefficient of solute element (M) with respect to an infinite dilute of one mass% state; and calculated by the classical Wagner formalism, as shown in **Eq. 14**. Where E_M^j was the first-interaction parameter and r_M^j was the second-interaction parameter (Hino, 2009), which are listed in **Table 3**.

$$a_M = f_M \times [\%M] \tag{13}$$

$$\lg f_M = \sum_{i=C,Si,Mn,P,S,MO,Al,Ti,O} \left(\left(e_M^i \times [\%i]\right) + \left(r_M^i \times [\%i]^2\right) + \left(r_M^{i,j} \times [\%i] \times [\%j]\right)\right) \tag{14}$$

$$r_{Al}^{O,Al} = \frac{-0.021 - 13.87}{T}, \quad r_{Al}^{Al,O} = 9.05$$

In addition, a_{MO_n} is the activity of the MOn in the slag with respect to the pure solid state and its values can be calculated by different methods (Guo, 2006; Zhang, 2007), including molecular theory, ion theory, regular ionic solution model, Factsage software and IMCT model. Although the chemical properties can be reflected by the molecular theory, the structural of the slag can not be expressed. The ion theory thought, the charge particles were consisted in and the complex molecules was regarded as charged ion clusters. The thermodynamic data of BaO-TiO_2 system (Barin, 1995; Lu and Jin, 2001; Ye, 2002; Cheng, 2010; Sahu et al., 2018) were not considered in the Factsage software (Bale et al., 2009). Therefore, it is necessary to established the IMCT model to calculate the activity of MO_n in the slag due to its satisfying the essence of slag structure.

IMCT MODEL DESCRIPTION

Establishment of the IMCT Model for $CaO-MgO-BaO-CaF_2-SiO_2-Al_2O_3-TiO_2$ Slag

According to the IMCT hypotheses proposed by literature (Zaitsev et al., 1990; Li and Zhang, 2000; Zhang, 2004; Zhang, 2007; Yang et al., 2009) and phase diagrams (Eisenhüttenleute, 1995; Shukla, 2012; Boulay et al., 2014), there are 4 simple cation-anion couples, 3 simple molecules and 51 complex molecules in this model at 1800–1935K, as shown in **Table 4**. The mole fraction of theses studied slag's components is assigned as a1 = $\sum n_{CaO}$, a2 = $\sum n_{MgO}$, a3 = $\sum n_{BaO}$, a4 = $\sum n_{CaF_2}$, a5 = $\sum n_{SiO_2}$,a6 = $\sum n_{Al_2O_3}$,a7 = $\sum n_{TiO_2}$. The equilibrium mole numbers and mass action concentrations of all structural units in CaO-MgO-BaO-CaF2-SiO2-Al2O3-TiO2 slag are listed in **Table 4**. The chemical reaction equations of all structural units in CaO-MgO-BaO-CaF2-SiO2-Al2O3-TiO2 slag are summarized in **Table 5**. The standard molar Gibbs free energy changes ΔG_i^0 and mass action concentrations expressed by Ki of this model's complex molecules structural units are also listed in **Table 5**.

According to the definition of mass action concentration and mass conservation, **Eq. 15–22** can be obtained, which could be solved with Matlab.

$$a_1 = \Big(0.5N_1 + N_8 + 2N_9 + 3N_{10} + N_{18} + N_{19} + N_{20} + 12N_{21} + 3N_{22} + N_{28} + 3N_{29} + 4N_{30} + 2N_{39} + N_{40} + N_{41} + N_{42} + N_{43} + 2N_{44} + 3N_{45} + 3N_{47} + 11N_{48} + 3N_{49}\Big)\sum n_i = \sum n_{CaO} \tag{15}$$

$$a_2 = (0.5N_2 + N_{12} + 2N_{13} + N_{23} + 2N_{31} + N_{32} + N_{33} + N_{42} + N_{43} + N_{44} + N_{45} + 2N_{46})\sum n_i = \sum n_{MgO} \tag{16}$$

$$a_3 = \Big(0.5N_3 + N_{14} + 2N_{15} + 2N_{16} + N_{17} + N_{24} + N_{25} + 3N_{26} + 2N_{34} + N_{35} + 4N_{36} + N_{37} + 2N_{38} + N_{50} + 2N_{51} + N_{52} + 3N_{53} + N_{54} + N_{55} + N_{56} + N_{57} + 2N_{58}\Big)\sum n_i = \sum n_{BaO} \tag{17}$$

$$a_4 = \Big(\frac{1}{3}N_4 + N_{47} + N_{48} + N_{49}\Big)\sum n_i = \sum n_{CaF_2} \tag{18}$$

$$a_5 = \Big(N_5 + N_8 + N_9 + N_{10} + 2N_{11} + N_{12} + N_{13} + N_{14} + N_{15} + 3N_{16} + 2N_{17} + N_{39} + 2N_{40} + N_{41} + N_{42} + 2N_{43} + 2N_{44} + 2N_{45} + 5N_{46} + 2N_{49} + 2N_{50} + 3N_{51} + 2N_{54} + 4N_{55} + 3N_{56} + 2N_{57} + 2N_{58}\Big)\sum n_i = \sum n_{SiO_2} \tag{19}$$

$$a_6 = \Big(N_6 + 3N_{11} + 6N_{18} + 2N_{19} + N_{20} + 7N_{21} + N_{22} + N_{23} + 6N_{24} + N_{25} + N_{26} + N_{27} + N_{39} + N_{40} + 2N_{46} + 3N_{47} + 7N_{48} + 4N_{52} + N_{53} + N_{54}\Big)\sum n_i = \sum n_{Al_2O_3} \tag{20}$$

$$a_7 = \Big(N_7 + N_{27} + N_{28} + 2N_{29} + 3N_{30} + N_{31} + N_{32} + 2N_{33} + 9N_{34} + 4N_{35} + 13N_{36} + N_{37} + N_{38} + N_{41} + N_{55} + N_{56} + N_{57} + N_{58}\Big)\sum n_i = \sum n_{TiO_2} \tag{21}$$

$$N_1 + N_2 + N_3 + N_4 + N_5 + N_6 + \ldots\ldots + N_{54} + N_{55} + N_{56} + N_{57} = \sum N_i = 1 \tag{22}$$

The Validation of IMCT Model for $CaO-MgO-BaO-CaF_2-SiO_2-Al_2O_3-TiO_2$ Slag

According to **Eq. 8** and **Eq. 12**, the dependence of the activity ratio of steel on the activity ratio of slag at different experiment heats, which includes JY. Li's (Li and Cheng, 2019), ZH. Jian's (Jiang et al., 2016),J.Park's (Park et al., 2008) and this author's experiment data, are shown in **Figure 2**. The activity of SiO_2, Al_2O_3 and TiO_2 in the slag are calculated by the IMCT model according to the final slag composition and the activity of Si, Al and Ti in the steel calculated by **Eq. 13** and **Eq. 14** according to the final steel composition, at different experiment heats. The magenta lines in this Figure are derived From **Eq. 8** and **Eq. 12**. And we can find that the activity of the slag calculated by IMCT Model are approved by the experiments.

The data of blue sphere is calculated by using this author's experiment results as shown in **Table 6** and the experiment method is described in **Table 7**. The CaO-MgO-BaO-CaF2-SiO2-Al2 O3-TiO2 slags before reacting with steel were pre-melted in a carbon crucible and the composition was shown in **Table 8**, which are marked as No.1~No.13. The steel sample A, described in **Table 1**, and the pre-melted CaO-MgO-BaO-CaF2-SiO2-Al2O3-TiO2 slags were equilibrated in MgO crucible by using resistance furnace under Ar atmosphere for 1 h.

The detailed process of slag/metal experiment can be described as follows. At first, 400 g steel were placed in a MgO crucible. Then, the slag/metal reaction chamber was filled by Ar gas and followed by resistance heating. After temperature reached 1873K, the initial steel sample was taken by quartz tube and then 32 g pre-melted slag was added. After the slag was melted at 1873K for 60 min, steel sample and slag sample were taken out. During the metal-slag reacting process, the steel sample were taken at 5, 20 and 40min after slag melting completely. The contents of silicon, soluble aluminum, titanium in steel samples were measured by the inductively coupled plasma optical emission spectrometry (ICP-OES) with ±5% relative standard

TABLE 4 | The kinds of structural units in this model, and their definition mole number and mass action concentration.

Item	Structural units as ion couples or molecules	Mole number of structure unit	Mass action concentration of structural unit or ion couples
Simple cation and anion	$(Ca^{2+}+O^{2-})$	$n_1 = 2n_{CaO}$	$N_1 = n_1/\sum n_i$
	$(Mg^{2+}+O^{2-})$	$n_2 = 2n_{MgO}$	$N_2 = n_2/\sum n_i$
	$(Ba^{2+}+O^{2-})$	$n_3 = 2n_{BaO}$	$N_3 = n_3/\sum n_i$
	$(Ca^{2+}+2F^{-})$	$n_4 = 3n_{CaF_2}$	$N_4 = n_4/\sum n_i$
Simple molecules	SiO_2	$n_5 = n_{SiO_2}$	$N_5 = n_5/\sum n_i$
	Al_2O_3	$n_6 = n_{Al_2O_3}$	$N_6 = n_6/\sum n_i$
	TiO_2	$n_7 = n_{TiO_2}$	$N_7 = n_7/\sum n_i$
Complex Molecules	$CaO{\cdot}SiO_2$	n_8	$N_8 = n_8/\sum n_i$
	$2CaO{\cdot}SiO_2$	n_9	$N_9 = n_9/\sum n_i$
	$3CaO{\cdot}SiO_2$	n_{10}	$N_{10} = n_{10}/\sum n_i$
	$3Al_2O_3{\cdot}2SiO_2$	n_{11}	$N_{11} = n_{11}/\sum n_i$
	$MgO{\cdot}SiO_2$	n_{12}	$N_{12} = n_{12}/\sum n_i$
	$2MgO{\cdot}SiO_2$	n_{13}	$N_{13} = n_{13}/\sum n_i$
	$2BaO{\cdot}SiO_2$	n_{14}	$N_{14} = n_{14}/\sum n_i$
	$BaO{\cdot}SiO_2$	n_{15}	$N_{15} = n_{15}/\sum n_i$
	$2BaO{\cdot}3SiO_2$	n_{16}	$N_{16} = n_{16}/\sum n_i$
	$BaO{\cdot}2SiO_2$	n_{17}	$N_{17} = n_{17}/\sum n_i$
	$CaO{\cdot}6Al_2O_3$	n_{18}	$N_{18} = n_{18}/\sum n_i$
	$CaO{\cdot}2Al_2O_3$	n_{19}	$N_{19} = n_{19}/\sum n_i$
	$CaO{\cdot}Al_2O_3$	n_{20}	$N_{20} = n_{20}/\sum n_i$
	$12CaO{\cdot}7Al_2O_3$	n_{21}	$N_{21} = n_{21}/\sum n_i$
	$3CaO{\cdot}Al_2O_3$	n_{22}	$N_{22} = n_{22}/\sum n_i$
	$MgO{\cdot}Al_2O_3$	n_{23}	$N_{23} = n_{23}/\sum n_i$
	$BaO{\cdot}6Al_2O_3$	n_{24}	$N_{24} = n_{24}/\sum n_i$
	$BaO{\cdot}Al_2O_3$	n_{25}	$N_{25} = n_{25}/\sum n_i$
	$3BaO{\cdot}Al_2O_3$	n_{26}	$N_{26} = n_{26}/\sum n_i$
	$Al_2O_3{\cdot}TiO_2$	n_{27}	$N_{27} = n_{27}/\sum n_i$
	$CaO{\cdot}TiO_2$	n_{28}	$N_{28} = n_{28}/\sum n_i$
	$3CaO{\cdot}2TiO_2$	n_{29}	$N_{29} = n_{29}/\sum n_i$
	$4CaO{\cdot}3TiO_2$	n_{30}	$N_{30} = n_{30}/\sum n_i$
	$2MgO{\cdot}TiO_2$	n_{31}	$N_{31} = n_{31}/\sum n_i$
	$MgO{\cdot}TiO_2$	n_{32}	$N_{32} = n_{32}/\sum n_i$
	$MgO{\cdot}2TiO_2$	n_{33}	$N_{33} = n_{33}/\sum n_i$
	$2BaO{\cdot}9TiO_2$	n_{34}	$N_{34} = n_{34}/\sum n_i$
	$BaO{\cdot}4TiO_2$	n_{35}	$N_{35} = n_{35}/\sum n_i$
	$4BaO{\cdot}13TiO_2$	n_{36}	$N_{36} = n_{36}/\sum n_i$
	$BaO{\cdot}TiO_2$	n_{37}	$N_{37} = n_{37}/\sum n_i$
	$2BaO{\cdot}TiO_2$	n_{38}	$N_{38} = n_{38}/\sum n_i$
	$2CaO{\cdot}Al_2O_3{\cdot}SiO_2$	n_{39}	$N_{39} = n_{39}/\sum n_i$
	$CaO{\cdot}Al_2O_3{\cdot}2SiO_2$	n_{40}	$N_{40} = n_{40}/\sum n_i$
	$CaO{\cdot}SiO_2{\cdot}TiO_2$	n_{41}	$N_{41} = n_{41}/\sum n_i$
	$CaO{\cdot}MgO{\cdot}SiO_2$	n_{42}	$N_{42} = n_{42}/\sum n_i$
	$CaO{\cdot}MgO{\cdot}2SiO_2$	n_{43}	$N_{43} = n_{43}/\sum n_i$
	$2CaO{\cdot}MgO{\cdot}2SiO_2$	n_{44}	$N_{44} = n_{44}/\sum n_i$
	$3CaO{\cdot}MgO{\cdot}2SiO_2$	n_{45}	$N_{45} = n_{45}/\sum n_i$
	$2MgO{\cdot}2Al_2O_3{\cdot}5SiO_2$	n_{46}	$N_{46} = n_{46}/\sum n_i$
	$3CaO{\cdot}3Al_2O_3{\cdot}CaF_2$	n_{47}	$N_{47} = n_{47}/\sum n_i$
	$11CaO{\cdot}7Al_2O_3{\cdot}CaF_2$	n_{48}	$N_{48} = n_{48}/\sum n_i$
	$3CaO{\cdot}2SiO_2{\cdot}CaF_2$	n_{49}	$N_{49} = n_{49}/\sum n_i$
	$BaO{\cdot}3CaO{\cdot}2SiO_2$	n_{50}	$N_{50} = n_{50}/\sum n_i$
	$2BaO{\cdot}4CaO{\cdot}3SiO_2$	n_{51}	$N_{51} = n_{51}/\sum n_i$
	$BaO{\cdot}2CaO{\cdot}4Al_2O_3$	n_{52}	$N_{52} = n_{52}/\sum n_i$
	$3BaO{\cdot}CaO{\cdot}Al_2O_3$	n_{53}	$N_{53} = n_{53}/\sum n_i$
	$BaO{\cdot}Al_2O_3{\cdot}2SiO_2$	n_{54}	$N_{54} = n_{54}/\sum n_i$
	$BaO{\cdot}4SiO_2{\cdot}TiO_2$	n_{55}	$N_{55} = n_{55}/\sum n_i$
	$BaO{\cdot}3SiO_2{\cdot}TiO_2$	n_{56}	$N_{56} = n_{56}/\sum n_i$
	$BaO{\cdot}2SiO_2{\cdot}TiO_2$	n_{57}	$N_{57} = n_{57}/\sum n_i$
	$2BaO{\cdot}2SiO_2{\cdot}TiO_2$	n_{58}	$N_{58} = n_{58}/\sum n_i$

TABLE 5 | The chemical reaction formulas of complex molecular in this model, and their Standard Molar Gibbs Free Energy Changes and Mass Action Concentrations of complex molecules expressed by K_i.

Reactions	ΔG_i^0	N_i	References
$(Ca^{2+}+O^{2-})+(SiO_2)=(CaO\cdot SiO_2)$	-81416-10.498T	$N_8 = K_1N_1N_5$	Zhang, (2007)
$2(Ca^{2+}+O^{2-})+(SiO_2)=(2CaO\cdot SiO_2)$	-160431 + 4.160T	$N_9 = K_2N_1^2N_5$	Zhang, (2007)
$3(Ca^{2+}+O^{2-})+(SiO_2)=(3CaO\cdot SiO_2)$	-92366-23.027T	$N_{10} = K_3N_1^3N_5$	Zhang, (2007)
$3(Al_2O_3)+2(SiO_2)=(3Al_2O_3\cdot 2SiO_2)$	8589.9-17.39T	$N_{11} = K_4N_6^3N_5^2$	Zhang, (2007)
$(Mg^{2+}+O^{2-})+(SiO_2)=(MgO\cdot SiO_2)$	43400-40.T	$N_{12} = K_5N_2N_5$	Zhang, (2007)
$2(Mg^{2+}+O^{2-})+(SiO_2)=(2MgO\cdot SiO_2)$	-77403 + 11.0T	$N_{13} = K_6N_2^2N_5$	Zhang, (2007)
$(Ba^{2+}+O^{2-})+(SiO_2)=(BaO\cdot SiO_2)$	-148950-6.28T	$N_{14} = K_7N_3N_5$	Bale et al. (2009)
$2(Ba^{2+}+O^{2-})+(SiO_2)=(2BaO\cdot SiO_2)$	-259826-5.86T	$N_{15} = K_8N_3^2N_5$	Bale et al. (2009)
$2(Ba^{2+}+O^{2-})+3(SiO_2)=(2BaO\cdot 3SiO_2)$	-337580 + 7.03T	$N_{16} = K_9N_3^2N_5^3$	Bale et al. (2009)
$(Ba^{2+}+O^{2-})+2(SiO_2)=(BaO\cdot 2SiO_2)$	-169365 + 1.49T	$N_{17} = K_{10}N_3N_5^2$	Bale et al. (2009)
$(Ca^{2+}+O^{2-})+6(Al_2O_3)=(CaO\cdot 6Al_2O_3)$	-17430-37.2T	$N_{18} = K_{11}N_1N_6^6$	Zhang, (2007)
$(Ca^{2+}+O^{2-})+2(Al_2O_3)=(CaO\cdot 2Al_2O_3)$	-16400-26.8T	$N_{19} = K_{12}N_1N_6^2$	Zhang, (2007)
$(Ca^{2+}+O^{2-})+(Al_2O_3)=(CaO\cdot Al_2O_3)$	-18120-18.62T	$N_{20} = K_{13}N_1N_6$	Zhang, (2007)
$12(Ca^{2+}+O^{2-})+7(Al_2O_3)=(12CaO\cdot 7Al_2O_3)$	-86100-205.1T	$N_{21} = K_{14}N_1^{12}N_6^7$	Zhang, (2007)
$3(Ca^{2+}+O^{2-})+(Al_2O_3)=(3CaO\cdot Al_2O_3)$	-17000-32.0T	$N_{22} = K_{15}N_1^3N_6$	Zhang, (2007)
$(Mg^{2+}+O^{2-})+(Al_2O_3)=(MgO\cdot Al_2O_3)$	-35530-2.09T	$N_{23} = K_{16}N_2N_6$	Zhang, (2007)
$(Ba^{2+}+O^{2-})+6(Al_2O_3)=(BaO\cdot 6Al_2O_3)$	-126813-24.29T	$N_{24} = K_{17}N_3N_6^6$	Bale et al. (2009)
$(Ba^{2+}+O^{2-})+(Al_2O_3)=(BaO\cdot Al_2O_3)$	-124264-6.694T	$N_{25} = K_{18}N_3N_6$	Bale et al. (2009)
$3(Ba^{2+}+O^{2-})+(Al_2O_3)=(3BaO\cdot Al_2O_3)$	-212125-18.83T	$N_{26} = K_{19}N_3^3N_6$	Bale et al. (2009)
$(Al_2O_3)+(TiO_2)=(Al_2O_3\cdot TiO_2)$	-25271 + 3.93T	$N_{27} = K_{20}N_6N_7$	Cheng, (2010); Jiang et al. (2016); Li and Cheng, (2019)
$(Ca^{2+}+O^{2-})+(TiO_2)=(CaO\cdot TiO_2)$	-74392-10.13T	$N_{28} = K_{21}N_1N_7$	Cheng, (2010); Jiang et al. (2016); Li and Cheng, (2019)
$3(Ca^{2+}+O^{2-})+2(TiO_2)=(3CaO\cdot 2TiO_2)$	-148365-24.14T	$N_{29} = K_{22}N_1^3N_7^2$	Cheng, (2010); Jiang et al. (2016); Li and Cheng, (2019)
$4(Ca^{2+}+O^{2-})+3(TiO_2)=(4CaO\cdot 3TiO_2)$	-292880-17.57T	$N_{30} = K_{23}N_1^4N_7^3$	Cheng, (2010); Jiang et al. (2016); Li and Cheng, (2019)
$2(Mg^{2+}+O^{2-})+(TiO_2)=(2MgO\cdot TiO_2)$	-25500 + 1.26T	$N_{31} = K_{24}N_2^2N_7$	Cheng, (2010); Jiang et al. (2016); Li and Cheng, (2019)
$(Mg^{2+}+O^{2-})+(TiO_2)=(MgO\cdot TiO_2)$	-26400 + 3.14T	$N_{32} = K_{25}N_2N_7$	Cheng, (2010); Jiang et al. (2016); Li and Cheng, (2019)
$(Mg^{2+}+O^{2-})+2(TiO_2)=(MgO\cdot 2TiO_2)$	-27600 + 0.63T	$N_{33} = K_{26}N_2N_7^2$	Cheng, (2010); Jiang et al. (2016); Li and Cheng, (2019)
$2(Ba^{2+}+O^{2-})+9(TiO_2)=(2BaO\cdot 9TiO_2)$	-406802 + 40.53T	$N_{34} = K_{27}N_3^2N_7^9$	Lu and Jin, (2001)
$(Ba^{2+}+O^{2-})+4(TiO_2)=(BaO\cdot 4TiO_2)$	-194314 + 14.87T	$N_{35} = K_{28}N_3N_7^4$	Lu and Jin, (2001)
$4(Ba^{2+}+O^{2-})+13(TiO_2)=(4BaO\cdot 13TiO_2)$	-74326 + 49.07T	$N_{36} = K_{29}N_3^4N_7^{13}$	Lu and Jin, (2001)
$(Ba^{2+}+O^{2-})+(TiO_2)=(BaO\cdot TiO_2)$	-166210 + 14.14T	$N_{37} = K_{30}N_3N_7$	Yang et al. (2009)
$2(Ba^{2+}+O^{2-})+(TiO_2)=(2BaO\cdot TiO_2)$	-202924-T	$N_{38} = K_{31}N_3^2N_7$	Yang et al. (2009)
$2(Ca^{2+}+O^{2-})+(Al_2O_3)+(SiO_2)=(2CaO\cdot Al_2O_3\cdot SiO_2)$	-17092 + 8.778T	$N_{39} = K_{32}N_1^2N_6N_5$	Zhang, (2007)
$(Ca^{2+}+O^{2-})+(Al_2O_3)+2(SiO_2)=(CaO\cdot Al_2O_3\cdot 2SiO_2)$	28006-74.195T	$N_{40} = K_{33}N_1N_6N_5^2$	Zhang, (2007)
$(Ca^{2+}+O^{2-})+(SiO_2)+(TiO_2)=(CaO\cdot SiO_2\cdot TiO_2)$	-114683 + 7.32T	$N_{41} = K_{34}N_1N_5N_7$	Cheng, (2010); Jiang et al. (2016); Li and Cheng, (2019)
$(Ca^{2+}+O^{2-})+(Mg^{2+}+O^{2-})+(SiO_2)=(CaO\cdot MgO\cdot SiO_2)$	-124766 + 3.768T	$N_{42} = K_{35}N_1N_2N_5$	Zhang, (2007)
$(Ca^{2+}+O^{2-})+(Mg^{2+}+O^{2-})+2(SiO_2)=(CaO\cdot MgO\cdot 2SiO_2)$	-80387-51.916T	$N_{43} = K_{36}N_1N_2N_5^2$	Zhang, (2007)
$2(Ca^{2+}+O^{2-})+(Mg^{2+}+O^{2-})+2(SiO_2)=(2CaO\cdot MgO\cdot 2SiO_2)$	-73668-63.639T	$N_{44} = K_{37}N_1^2N_2N_5^2$	Zhang, (2007)
$3(Ca^{2+}+O^{2-})+(Mg^{2+}+O^{2-})+2(SiO_2)=(3CaO\cdot MgO\cdot 2SiO_2)$	-315469 + 24.786T	$N_{45} = K_{38}N_1^3N_2N_5^2$	Zhang, (2007)
$2(Mg^{2+}+O^{2-})+2(Al_2O_3)+5(SiO_2)=(2MgO\cdot 2Al_2O_3\cdot 5SiO_2)$	-14422-14.808T	$N_{46} = K_{39}N_2^2N_6^2N_5^5$	Zhang, (2007)
$3(Ca^{2+}+O^{2-})+3(Al_2O_3)+(Ca^{2+}+2F^{-})=(3CaO\cdot 3Al_2O_3\cdot CaF_2)$	-44492-73.15T	$N_{47} = K_{40}N_1^3N_6^3N_4$	Cheng, (2010); Jiang et al. (2016); Li and Cheng, (2019)
$11(Ca^{2+}+O^{2-})+7(Al_2O_3)+(Ca^{2+}+2F^{-})=(11CaO\cdot 7Al_2O_3\cdot CaF_2)$	-228760-155.8T	$N_{48} = K_{41}N_1^{11}N_7^7N_4$	Cheng, (2010); Jiang et al. (2016); Li and Cheng, (2019)
$3(Ca^{2+}+O^{2-})+2(SiO_2)+(Ca^{2+}+2F^{-})=(3CaO\cdot 2SiO_2\cdot CaF_2)$	-255180-8.2T	$N_{49} = K_{42}N_1^3N_5^2N_4$	Cheng, (2010); Jiang et al. (2016); Li and Cheng, (2019)
$(Ba^{2+}+O^{2-})+3(Ca^{2+}+O^{2-})+2(SiO_2)=(BaO\cdot 3CaO\cdot 2SiO_2)$	-376298 + 8.75T	$N_{50} = K_{43}N_3N_1^3N_5^2$	Bale et al. (2009)
$2(Ba^{2+}+O^{2-})+4(Ca^{2+}+O^{2-})+3(SiO_2)=(2BaO\cdot 4CaO\cdot 3SiO_2)$	-533550 + 269.29T	$N_{51} = K_{44}N_3N_1^4N_5^3$	Bale et al. (2009)
$(Ba^{2+}+O^{2-})+2(Ca^{2+}+O^{2-})+4(Al_2O_3)=(BaO\cdot 2CaO\cdot 4Al_2O_3)$	-157255-85.11T	$N_{52} = K_{45}N_3N_1^2N_6^4$	Bale et al. (2009)
$3(Ba^{2+}+O^{2-})+(Ca^{2+}+O^{2-})+(Al_2O_3)=(3BaO\cdot CaO\cdot Al_2O_3)$	-139905-42.19T	$N_{53} = K_{46}N_3^3N_1N_6$	Bale et al. (2009)
$(Ba^{2+}+O^{2-})+(Al_2O_3)+2(SiO_2)=(BaO\cdot Al_2O_3\cdot 2SiO_2)$	-198791-38.49T	$N_{54} = K_{47}N_3N_6N_5^2$	Bale et al. (2009)
$(Ba^{2+}+O^{2-})+4(SiO_2)+(TiO_2)=(BaO\cdot 4SiO_2\cdot TiO_2)$	-291417-72.91T	$N_{55} = K_{48}N_3N_5^4N_7$	Barin, (1995); Ye, (2002); Sahu et al. (2018)
$(Ba^{2+}+O^{2-})+3(SiO_2)+(TiO_2)=(BaO\cdot 3SiO_2\cdot TiO_2)$	-284166-55.31T	$N_{56} = K_{49}N_3N_5^3N_7$	Barin, (1995); Ye, (2002); Sahu et al. (2018)
$(Ba^{2+}+O^{2-})+2(SiO_2)+(TiO_2)=(BaO\cdot 2SiO_2\cdot TiO_2)$	-249835-59.44T	$N_{57} = K_{50}N_3N_5^2N_7$	Barin, (1995); Ye, (2002); Sahu et al. (2018)
$2(Ba^{2+}+O^{2-})+2(SiO_2)+(TiO_2)=(2BaO\cdot 2SiO_2\cdot TiO_2)$	-458720-7.14T	$N_{58} = K_{51}N_3^2N_5^2N_7$	Barin, (1995); Ye, (2002); Sahu et al. (2018)

deviation. The compositions of slag samples were measured by an X-ray fluorescence spectrometer. During the metal-slag reacting process, the composition change behavior of the silicon in the steel was shown in **Figure 3**. From **Figure 3**, the experiment equilibrium state has realized.

In addition, the activity of SiO_2, Al_2O_3 and TiO_2 in 2–5 dimensional slag from the literature (Gzieo and Jowsa, 1984; Nomura et al., 1991; Hino, 1994; Kishi et al., 1994; Ohta and Suito, 1994; Ohta and Suito, 1998a; Ohta and Suito, 1998b; Moeizane et al., 1999; Jung and Fruehan, 2001; Stolyarova

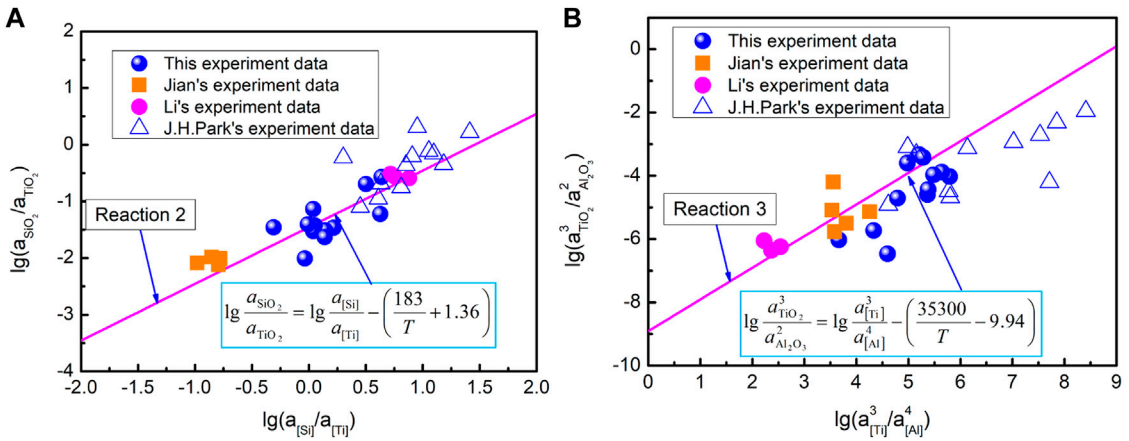

FIGURE 2 | The relationship between the activity ratio of steel and the activity ratio of slag in the experiment.

TABLE 6 | This author's experiment result (wt pct).

NO.	CaO	MgO	BaO	CaF2	SiO2	Al2O3	TiO2	[Ti]	[Al]	[Si]
1	40.5	8.8	3.2	3.9	5.2	20.2	18.2	0.128	0.009	0.186
2	35.1	9.3	9.1	4.5	4.3	19.7	17.8	0.169	0.011	0.208
3	28.6	8.3	14.7	5.3	4.3	20.1	18.5	0.232	0.011	0.232
4	28.3	7.7	18.3	4.9	4.1	15.4	21.3	0.24	0.018	0.233
5	46.3	7.8	0	4.4	4.4	17.8	19.3	0.178	0.016	0.217
6	49.6	8.4	0	4.5	15.1	17.4	5.0	0.091	0.018	0.345
7	37.0	10.5	0	4.2	7.8	35.9	4.6	0.083	0.010	0.23
8	40.9	12.0	0	4.0	7.6	26.7	8.6	0.133	0.011	0.245
9	33.8	11.7	0	3.9	7.0	23.4	20.4	0.206	0.011	0.20
10	34.0	-	19.05	5.52	5.25	14.62	21.26	0.506	0.024	0.228
11	30.81	-	19.88	4.10	4.66	14.00	26.55	0.264	0.017	0.231
12	33.63	-	20.38	4.98	2.08	10.64	28.30	0.235	0.015	0.193

TABLE 7 | This author's experiment methods.

Experiment heats	Temperature (K)	Atmosphere	Crucible	Steel (g)	Slag	Time
Resistance furnace	1873	Ar	MgO	400	32 g pre-melted slags	1 h

TABLE 8 | The initial slag composition (%).

No	CaO	MgO	BaO	CaF2	SiO2	Al2O3	TiO2
1	43.7	6.0	6.0	5.0	4.0	20.3	15.0
2	36.7	6.0	13.0	5.0	4.0	20.3	15.0
3	29.7	6.0	20.0	5.0	4.0	20.3	15.0
4	30.0	6.0	20.0	5.0	4.0	15.0	20.0
5	49.7	6.0	0	5.0	4.0	20.3	15.0
6	54.0	6.0	0	5.0	18.0	17.0	0
7	42.0	6.0	0	5.0	8.0	39.0	0
8	46.8	6.0	0	5.0	8.0	29.2	5.0
9	37.5	6.0	0	5.0	8.0	23.5	20.0
10	34.43		19.13	4.55	6.00	15.28	20.61
11	31.61		20.39	4.43	5.01	14.44	24.11
12	35.25		21.36	5.19	1.51	11.26	25.43

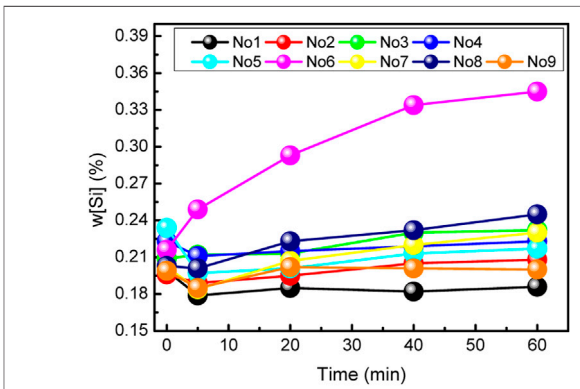

FIGURE 3 | The Silicon content of the steel in different heats.

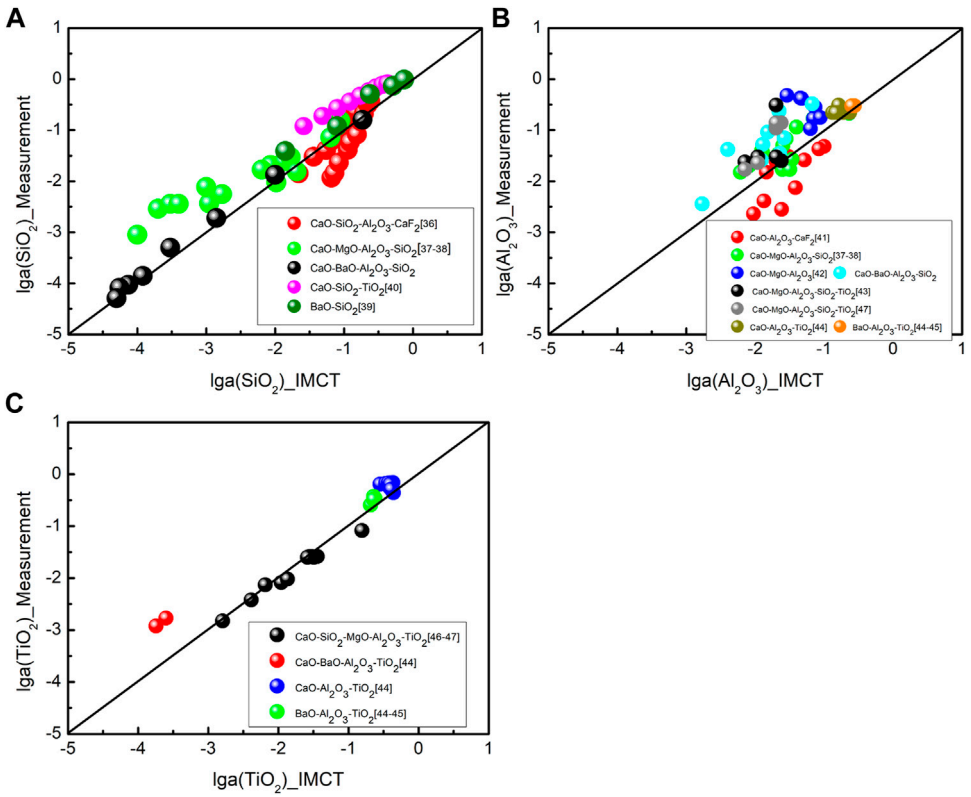

FIGURE 4 | The comparison of specie's activity in slag between measured and calculated values. **(A)** The activity of SiO_2; **(B)** The activity of Al_2O_3; **(C)** The activity of TiO_2.

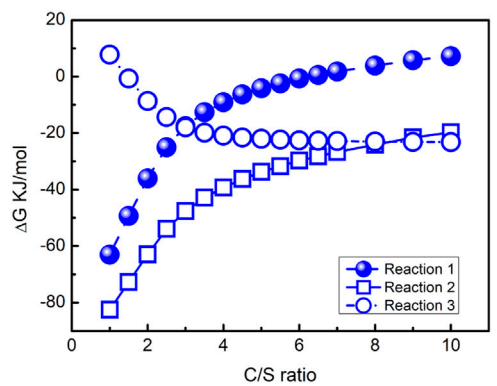

FIGURE 5 | The effect of C/S ratio on the ΔG of reactions 1–3.

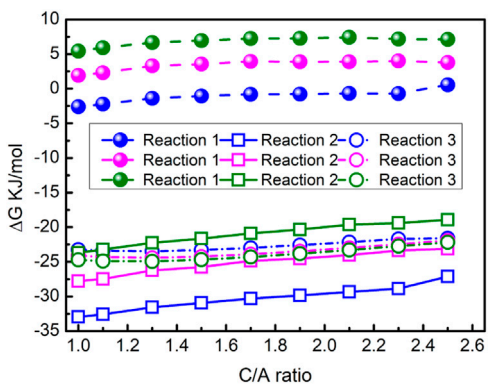

FIGURE 6 | The influence of C/A ratio on the ΔG of reactions 1–3.

et al., 2005; Sun et al., 2015; Safarin, 2019) are calculated by this paper's IMCT model, and compared with their experiment results (Gzieo and Jowsa, 1984; Nomura et al., 1991; Hino, 1994; Kishi et al., 1994; Ohta and Suito, 1994; Ohta and Suito, 1998a; Ohta and Suito, 1998b; Moeizane et al., 1999; Jung and Fruehan, 2001; Stolyarova et al., 2005; Sun et al., 2015; Safarin, 2019) and Factsage-7.0 calculating values, as shown in **Figure 4**. In **Figure 4A** or **Figure 4B**, the activity of SiO_2 or Al_2O_3 in the CaO-BaO-Al_2O_3-SiO_2 slag system calculated by the IMCT model are in good agreement with the Factsage-7.0 calculating values. It also can be found that, the activity of low system slag calculated by IMCT model are in accordance to the experimental results. In summary, the IMCT model for CaO-MgO-BaO-CaF_2-SiO_2-Al_2O_3-TiO_2 slag in this paper is reasonable.

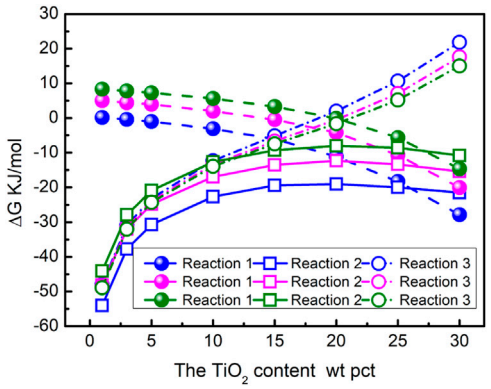

FIGURE 7 | The effect of TiO_2 content on the ΔG of reactions 1–3.

RESULT AND DISCUSSION

Influence of the C/S Ratio in the Slag

The dependence of C/S ratio in the slag (S1), listed in **Table 2**, on the ΔG of reactions 1–3 was shown in **Figure 5**. With the increase of C/S ratio in the slag, the ΔG of reactions 1–2 increased and the ΔG of reaction 3 decreased. In general, the C/S ratio in the slag was suggested to be higher 4 for Al-killed steel refining process. But Zhang et al. (Zhang, 2019) found that the C/S ratio of 6 was the most effective to improve the steel cleanliness. When the C/S ratio was higher 6, the ΔG of reaction 1 was higher than 0 kJ/mol and the ΔG of reactions 2–3 were about -25 kJ/mol, Therefore Ti in the steel will be oxidized by the SiO_2 and Al_2O_3 in the slag. Therefore it is necessary to investigate other factors such as C/A ratio, TiO_2 content and BaO content to suppress the re-oxidation of Ti by SiO_2 and Al_2O_3.

Influence of the C/A Ratio in the Slag

The effect of C/A ratio in the slag (S2), listed in **Table 2**, on the ΔG of reaction 1–3 is shown in **Figure 6**. In this figure, the blue symbol-line represents the C/S ration in the slag is 6, the magenta symbol-line means the C/S ratio is 8, and the olive symbol-line means the C/S ratio is 10. From this figure we can found that, when the C/A ratio changed from 1 to 2.5, the ΔG of reaction 2 and 3 are also lower -20 kJ/mol. Yoon et al. (Yoon et al., 2002) reported that the most effective C/A ratio in the high basicity slag, in which the C/S ratio was higher than 4, was 1.7–1.8 to removing inclusions from bearing steel. Therefore, the mass ratio of CaO to Al_2O_3 in the slag (S3 and S4) was 1.7 in the following discussion.

Influence of the w(TiO_2) in the Slag

Figure 7 shows the variation behavior of ΔG for reactions 1–3 with the increase of TiO_2 content in the slag (S3), listed in **Table2**. In this figure, the C/S ratio in the slag, marked in different color symbols, was the same with **Figure 6**. From **Figure 7**, with the increase of TiO_2 content in the slag, the ΔG of reaction 1 decreased, And the ΔG of reaction 2 and 3 increased. When the TiO_2 content in the slag was greater than 20%, the ΔG of reaction 2 are also lower than -10 kJ/mol. Therefore, it is necessary to increase the C/S ratio in the slag. However,

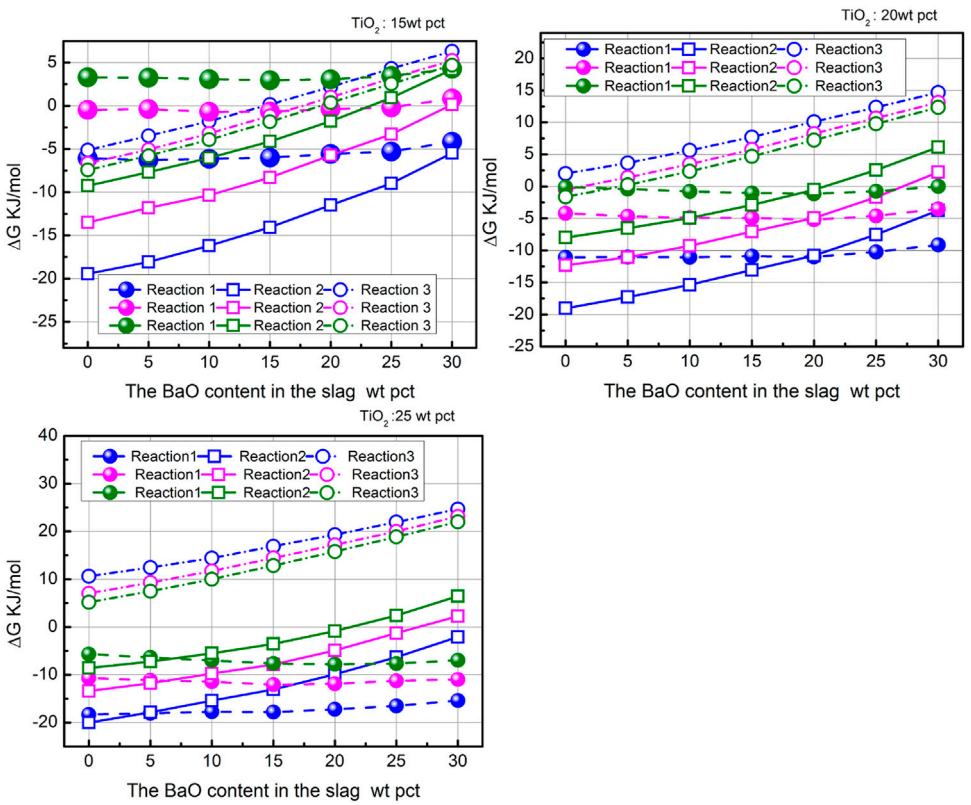

FIGURE 8 | The effect of BaO content on the ΔG of reactions 1–3.

the activity of CaO in the slag would increase and the solid calcium titanates (Li et al., 2018) would appear. This will lead to decrease the desulfurizer ability of the slag. In the basic slag TiO_2 exits as TiO_6^{8-} ions (Sommerville and Bell, 1982). In addition, TiO_2 in slag forms anions, which will cause free O^{2-} ions to decrease and the desulfurization ability of the slag decrease.

Influence of the BaO Content in the Slag

Figure 8 shows the influence of BaO content in the slag (S4) on the ΔG of reactions 1–3. In this figure, the C/S ratio in the slag, marked in different color symbols, was the same with **Figure 6**. It is clear that, the ΔG of reaction 1 changed less and the ΔG of reactions 2 and 3 increased with the addition of BaO to the slag. It is clear that from **Figure 8A**, when the slag contained 15%TiO_2, the C/S ratio was higher than 10 and the BaO content was 25–30%, the ΔG of reactions 1–3 are higher than 0 kJ/mol. When the TiO_2 content in the slag was higher than 20%, with the increase of BaO content in the slag, the ΔG of reaction 1 was still lower than 0. Therefore, when the BaO content and TiO_2 content in the slag were controlled as 20–30% and 15–25%, the C/S ratio should be controlled as higher than 10 according to the thermodynamic results. However, the desulfurizer and inclusion absorption ability of the slag should be considered. When the TiO_2 content was higher than 30%, a large amount of solid calcium titanates (Li et al., 2018) will formed in the slag, the viscosity of the slag increase. This would lead to the desulfurizer and inclusion absorption ability descend. BaO is more powerful desulfurizer than CaO. Adding BaO to the flux not only desulfurizers by itself, but also enhances the desulphurization ability of CaO. In addition, BaO is more inclined to release the oxygen ion for less affinity to oxygen than CaO, which also favors desulfurization. However, the increase of BaO content in the flux may lead to the decrease of molar fraction of basic components because of its high molecular mass (153). Also, BaS is not stable and tends to decompose with the increase of BaS, which is disadvantageous to the desulfurization reaction (Gao et al., 2012).

CONCLUSION

In this work, the thermodynamic interaction between ladle slag and 0.361%Ti bearing steel has been analyzed using IMCT model and the following conclusion are obtained.

1) According to the comparing results between thermodynamic calculation and experimental values, the IMCT model established in this paper is reasonable.
2) With the increase of C/S ratio in the slag, the ΔG of reaction for Al and Ti reacted with SiO_2 increased, and Ti reacted with Al_2O_3 decreased; the effect of C/A ratio in the slag on the change of ΔG for Al or Ti reacted with slag is less; with the addition of TiO_2 to the slag, the ΔG for Ti reacted with SiO_2 and Al_2O_3 increase, and Al reacted with SiO_2 decrease; with the increase of BaO in the slag, the ΔG change for reaction 1 is less, and the ΔG for reaction 2 and 3 increase.
3) When the BaO content and TiO_2 content in the slag were controlled as 20–30% and 15–25%, the C/S ratio should be controlled as higher than 10 according to the thermodynamic results. However, the desulphurization and inclusion absorption ability of the slag should be considered.

DATA AVAILABILITY STATEMENT

The original contributions presented in the study are included in the article/supplementary material, further inquiries can be directed to the corresponding author.

AUTHOR CONTRIBUTIONS

M-GZ was the first author and has made significant contribution to the manuscript. X-FW and G-JC have contributed towards the conception and review of the manuscript. S-PH provided correspondence and guidance on the manuscript.

FUNDING

The authors gratefully express their appreciation to National Natural Science Foundation of China (No.52074054) and the fourth batch of major science and technology projects in panxi experimental base (low cost manufacturing technique of titanium alloyed high-strength and hightoughness steel and its application).

REFERENCES

Bale, C. W., Bélisle, E., Chartrand, P., Decterov, S. A., Eriksson, G., Hack, K., et al. (2009). FactSage Thermochemical Software and Databases - Recent Developments. *Calphad* 33 (2), 295–311. doi:10.1016/j.calphad.2008.09.009

Barin, I. (1995). *Thermochemical Data of Pure Substances*. NewYork: VCH Publishers.

Bomberger, H. B., and Froes, F. H. (1984). The Melting of Titanium. *Jom* 36, 39–47. doi:10.1007/bf03339212

Boulay, E., Nakano, J., Turner, S., Idrissi, H., Schryvers, D., and Godet, S. (2014). Critical Assessments and Thermodynamic Modeling of BaO-SiO2 and SiO2-TiO2 Systems and Their Extensions into Liquid Immiscibility in the BaO-SiO2-TiO2 System. *Calphad* 47, 68–82. doi:10.1016/j.calphad.2014.06.004

Carmack, W. J., Smolik, G. R., and Mccarthy, K. A. (1996). Electroslag Remelt Processing of Irradiated Vanadium Alloys. *J. Nucl. Mater.* 233-237, 416–420. doi:10.1016/s0022-3115(96)00228-0

Cavazos, J. L., Gomez, I., and Guerrero-Mata, M. P. (2011). Stabilisation of Ferritic Stainless Steels with Zr and Ti Additions. *Mater. Sci. Technol.* 27, 530–536. doi:10.1179/026708309x12506933873747

Cheng, J. X. (2010). *Steelmaking Commonly Used Chart Data Manual*. BeiJing: Metallurgical Industry Press.

Eisenhüttenleute, V. D. (1995). *Slag Atlas[M]*. Germany: Düsseldorf.

Fujimura, H., Tsuge, S., Komizo, Y., and Nishizawa, T. (2001). Effect of Oxide Composition on Solidification Structure of Ti Added Ferritic Stainless Steel. *Tetsu-to-Hagane* 87, 707–712. doi:10.2355/tetsutohagane1955.87.11_707

Gao, Y., Liu, Q., and Bian, L. (2012). Effect of Composition on Desulfurization Capacity in the CaO-SiO2-Al2O3-MgO-CaF2-BaO System. *Metall. Materi Trans. B* 43, 229–232. doi:10.1007/s11663-011-9607-1

Guo, H. J. (2006). *Metallurgical Physical Chemistry*. BeiJing: Metallurgical Industry Press.

Gzieo, A., and Jowsa, J. (1984). Activity of SiO2 in Slag CaO-SiO2-Al2O3-CaF2. *Archiwum Hutnictwa* 29, 319–331.

Hino, M. (1994). CAMP. *ISIJ* Vol. 7, 41.

Hino, M. (2009). *Thermodynamic Data for Steelmaking*. Sendai Japan: Tohoku University Press.

Huang, L., Deng, X., Jia, Y., Li, C., and Wang, Z. (2018). Effects of Using (Ti,Mo)C Particles to Reduce the Three-Body Abrasive Wear of a Low alloy Steel. *Wear* 410-411, 119–126. doi:10.1016/j.wear.2018.06.008

Jiang, Z.-H., Hou, D., Dong, Y.-W., Cao, Y.-L., Cao, H.-B., and Gong, W. (2016). Effect of Slag on Titanium, Silicon, and Aluminum Contents in Superalloy during Electroslag Remelting. *Metall. Materi Trans. B* 47, 1465–1474. doi:10.1007/s11663-015-0530-8

Jiang, Z. H. (2000). *The Physical Chemistry and Transmission during Electroslag Remelting*. Shenyang: Northeastern University Press.

Jung, S.-M., and Fruehan, R. J. (2001). Thermodynamics of Titanium Oxide in Ladle Slags. *ISIJ Int.* 41, 1447–1453. doi:10.2355/isijinternational.41.1447

Kim, D. S., Park, J. J., Song, H. S., Shin, Y. K., Choi, B. H., and Yim, S. S. "Iron and Steel Society. Steelmaking Division," in Proceedings of the 76th Steelmaking Conference, Warrendale, PA, 1993, 291–297.

Kishi, M., Ioue, R., and Suito, H. (1994). Thermodynamics of Oxygen and Nitrogen in Liquid Fe-20mass%Cr alloy Equilibrated with Titania-Based Slags. *ISIJ* 34, 859–867.

Leban, M. B., and Tisu, R. (2013). The Effect of TiN Inclusions and Deformation-Induced Martensite on the Corrosion Properties of AISI 321 Stainless Steel. *Eng. Fail. Anal.* 33, 430–438. doi:10.1016/j.engfailanal.2013.06.021

Li, J., and Cheng, G. (2019). Effect of CaO-MgO-SiO2-Al2O3-TiO2 Slags with Different CaF2 Contents on Inclusions in Ti-Stabilized 20Cr Stainless Steel. *ISIJ Int.* 59, 2013–2023. doi:10.2355/isijinternational.isijint-2019-277

Li, J., Ruan, G., Li, J., Pan, J., and Chen, X. (2018). Evolution Mechanism of Inclusions in Al-Killed, Ti-Bearing 11Cr Stainless Steel with Ca Treatment. *ISIJ Int.* 58, 1042–1051. doi:10.2355/isijinternational.isijint-2017-565

Li, J. X., and Zhang, J. (2000). Calculation Model on Viscosity of CaO-MgO-MnO-FeO-CaF2-Al2O3-SiO2 Slags. *J. Univ. Sci. Technol Beijing* 22, 438–441. doi:10.13374/j.issn1001-053x.2000.05.012

Li, Z. B. (2010). *Electroslag Metallurgy Theory and Practice*. Beijing: Metallurgical Industry Press.

Lu, X. G., and Jin, Z. P. (2001). Thermodynamic Assessment of the BaO-TiO2 Quasibinary System. *Calphad* 24, 319–338. doi:10.1016/S0364-5916(01)00008-6

Maddalena, R., Rastogi, R., El-Dasher, B., and Cramb, A. W. "Nozzle Deposits in Titanium Treated Stainless Steel," in 58th Electric Furnace Conf. and 17th Process Technology Conf. Proc.,Iron and Steel Society, London, 2000, 811–832.

Moeizane, Y., Ozturk, B., and Fruehan, R. J. (1999). Thermodynamics of TiOx in Blast Furnace-type Slags. *Metallurgical Mater. Trans. B* 30, 29–43.

Nomura, K., Ozturk, B., and Fruehan, R. J. (1991). Removal of Nitrogen from Steel Using Novel Fluxes. *Mtb* 22, 783–790. doi:10.1007/bf02651155

Nunnington, R. C., and Sutcliffe, N. "The Steelmaking and Casting of Ti Stabilized Stainless Steels," in Proceedings of the 59th Electric Furnace Conf. and 19th Process Technology Conference, Warrendale, PA, 2001, 361–394.

Ohta, H., and Suito, H. (1994). Activities in CaO-MgO-Al2O3 Slags and Deoxidation Equilibria of Al, Mg and Ca. *ISIJ.Int* 36, 983–990.

Ohta, H., and Suito, H. (1998). Activities of SiO2 and Al2O3 and Activity Coefficients of FetO and MnO in CaO-SiO2-Al2O3-MgO Slags. *Metall. Materi Trans. B* 29, 119–129. doi:10.1007/s11663-998-0014-1

Ohta, H., and Suito, H. (1998). Deoxidation Equilibria of Calcium and Magnesium in Liquid Iron. *Metallurgical Mater. Trans. B* 28, 1131–1139.

Park, D.-C., Jung, I.-H., Rhee, P. C. H., and Lee, H.-G. (2004). Reoxidation of Al-Ti Containing Steels by CaO-Al2O3-MgO-SiO2 Slag. *ISIJ Int.* 44, 1669–1678. doi:10.2355/isijinternational.44.1669

Park, J.-H., Lee, S.-B., Kim, D. S., and Pak, J.-J. (2009). Thermodynamics of Titanium Oxide in CaO-SiO2-Al2O3-MgOsatd-CaF2 Slag Equilibrated with Fe-11mass %Cr Melt. *ISIJ Int.* 49, 337–342. doi:10.2355/isijinternational.49.337

Park, J. H., Lee, S.-B., and Gaye, H. R. (2008). Thermodynamics of the Formation of MgO-Al2O3-TiO X Inclusions in Ti-Stabilized 11Cr Ferritic Stainless Steel. *Metall. Materi Trans. B* 39, 853–861. doi:10.1007/s11663-008-9172-4

Qian, G.-Y., Jiang, F., Cheng, G.-G., and Wang, C.-S. (2014). Effect of TiO2addition to LF Refining Slag on the Ti, Al, and Cleanliness of Ti-Stabilized Stainless Steel. *Metall. Res. Technol.* 111, 229–237. doi:10.1051/metal/2014029

Safarin, J. (2019). Thermochemical Aspects of boron and Phosphours Distribution between Silicon and CaO-BaO-SiO2 Slags. *SILICON* 11, 437–451. doi:10.1007/s12633-018-9919-8

Sahu, M., Mukherjee, S., Keskar, M., Krishnan, K., Dash, S., and Tomar, B. S. (2018). Investigations of Thermophysico-Chemical Properties of Ba 2 TiSi 2 O 8 (S) and Sr 2 TiSi 2 O 8 (S). *Thermochim. Acta* 663, 215–226. doi:10.1016/j.tca.2018.02.003

Shukla, A. (2012). *Development of a Critically Evaluated Thermodynamic Databse for the Systems Containing Alkaline-Earth Oxides*. Montreal, Canada: École Polytechnique de Montréal.

Sommerville, I. D., and Bell, H. B. (1982). The Behaviour of Titania in Metallurgical Slags. *Can. Metallurgical Q.* 21, 145–155. doi:10.1179/cmq.1982.21.2.145

Stolyarova, V. L., Opatin, S. I. L., and Plotnikov, E. N. (2005). Thermodynamic Properties and Vaporisation Processes of Ternary Glass Forming Silicate Systems: CaO-Al2O3-SiO2, CaO-TiO2-SiO2 and BaO-TiO2-SiO2. *Phys. Chem. glasses* 46, 119–127.

Sun, Y., Liu, Z. N., and Tao, D. P. (2015). Prediction of TiO2 Activity in Al2O3-CaO-MgO-SiO2-TiO2 Slag System by Molecular Interaction Volume Model. *J. Kunming Univ. Sci. Technology(Natural Sci. Edition)* 40, 1–9. doi:10.16112/j.cnki.53-1223/n.2015.05.001

Yang, X.-M., Jiao, J.-S., Ding, R.-C., Shi, C.-B., and Guo, H.-J. (2009). A Thermodynamic Model for Calculating Sulphur Distribution Ratio between CaO-SiO2-MgO-Al2O3 Ironmaking Slags and Carbon Saturated Hot Metal Based on the Ion and Molecule Coexistence Theory. *ISIJ Int.* 49, 1828–1837. doi:10.2355/isijinternational.49.1828

Ye, D. L. (2002). *Handbook of Practical Inorganic Thermodynamics*. BeiJing: Metallurgical Industry Press.

Yoon, B.-H., Heo, K.-H., Kim, J.-S., and Sohn, H.-S. (2002). Improvement of Steel Cleanliness by Controlling Slag Composition. *Ironmaking & Steelmaking* 29, 214–217. doi:10.1179/030192302225004160

Zaitsev, A. I., Korolyov, N. V., Mogutnov, B. M., and Vyatkin, Y. F. "Thermodynamic and Crystallization Model of Slag for Ladle Treatment of Steel," in Proceedings of the 6th International Iron Steel Congress, 1990 (Nagoya, 185–193.

Zhang, J. (2004). Application of Annexation Principle to the Study of Thermodynamic Properties of Ternary Molten Salts CaCl2-MgCl2-NaCl. *Rare Met.* 23, 209–213.

Zhang, J. (2007). *Thermodynamic Calculations of Metallurgical Melts and Solutions*. BeiJing: Metallurgical Industry Press.

Zhang, L. F. (2019). *Non-metallic Inclusions in Steel: Fundamentals*. BeiJing: Metallurgical Industry Press.

Zheng, H., Chen, W., and Hu, Y. "Iron and Steel Technology Conference," in Proceedings Iron & Steel Technology Conference. (AISTech 2004), Warrendale, PA, September 2004 (AISI), 397.

Conflict of Interest: The authors declare that the research was conducted in the absence of any commercial or financial relationships that could be construed as a potential conflict of interest.

Publisher's Note: All claims expressed in this article are solely those of the authors and do not necessarily represent those of their affiliated organizations, or those of the publisher, the editors and the reviewers. Any product that may be evaluated in this article, or claim that may be made by its manufacturer, is not guaranteed or endorsed by the publisher.

NOMENCLATURE

C/S ratio the mass ratio of $CaO\text{-}SiO_2$

C/Al ratio the mass ratio of $CaO\text{-}Al_2O_3$

ΔG_i^0 the standard molar Gibbs free energy change of reaction i, (J/mol)

ΔG_i the molar Gibbs free energy change of reaction i, (J/mol)

K_i the equilibrium constant of reaction i

f_i the activity coefficient of element i in the liquid steel.